Asymmetric Top Rotors in Electric Fields. II. Influence of Internal Torsions in Molecular Beam Deflection Experiments

R. Antoine,* M. Abd El Rahim, M. Broyer, D. Rayane, and Ph. Dugourd

Laboratoire de Spectrométrie Ionique et Moléculaire, UMR 5579 (Université Lyon I et CNRS), Bât. A. Kastler, 43 Bd du 11 Novembre 1918, 69622 Villeurbanne Cedex, France

Received: March 8, 2006; In Final Form: June 14, 2006

We report on electric deflection experiments of aminobenzonitrile and (dimethylamino)benzonitrile molecules. They are used as prototypes to study the influence of the asymmetry and rotation−vibration couplings in deflection experiments. Experimental deflection profiles are compared to results of ab initio calculations in the frame of the rigid rotor Stark effect and of the statistical linear response. The change in symmetry and the introduction of methyl groups lead to a transition from the rigid rotor response to the linear response. From the experimental results, a total dipole of $\mu = 6.2 \pm 0.6$ D has been deduced for the *m*-(dimethylamino)-benzonitrile molecule (MDMABN).

1. Introduction. Molecular beam deflections or manipulations of polar molecules with static fields are widely used. The response of the molecules to electric or magnetic fields strongly depends on their rotation motion and on its possible couplings with other molecular motion or potential terms.[1−8] We studied, in part I of this series of two articles,[9] the influence of the asymmetry of a molecule in electric deflection experiments. We investigated electric beam deflections of aminobenzonitrile (ABN) molecules, and we found, for asymmetric molecules, that the results were in poor agreement with the simulations obtained from the calculations of the rotational levels of the rigid rotor in the electric field. This disagreement was induced by perturbations to the rotational motion because of interactions with other particles (collisions with carrier gas or buffer gas) and was particularly important when the rotational motion of asymmetric rotors in an external field became chaotic.

In the absence of collisions, the effect of chaotic rotational motion can be enhanced by other perturbations such as inhomogeneous external fields, rotation−vibration couplings, and spin relaxation for magnetic deflections. The aim of this paper is to study experimentally the influence of rotation−vibration couplings on molecular deflections, to demonstrate the importance of the effect, and to provide a basis for a better understanding of electric and magnetic deflections of complex systems. These couplings could be prompted by increasing the temperature of the molecules[4,10] or by increasing the flexibility of the molecules. ABN molecules are rather rigid molecules; the first observed vibration mode in ABN molecules has a frequency of ∼400 cm^{-1},[11] and thus rotation−vibration couplings are expected to be ineffective at room temperature. An easy way to increase the flexibility of ABN molecules is to introduce hindered internal motion by replacing the amino group by a dimethylamino group.

In this paper, we present electric deflections of *p*- and *m*-aminobenzonitrile (PABN and MABN) and of *p*- and *m*-(dimethylamino)benzonitrile (PDMABN and MDMABN) molecules. These molecules have a large permanent electric dipole moment. From *para* to *meta*, the asymmetry of the molecule is increased. Because of methyl groups, the vibration frequency modes in DMABN molecules are much lower than in ABN molecules[12] and can be populated at room temperature.

2. Experiment. The experimental apparatus has been previously described.[9,13] It consists of a molecular beam source coupled to an electric deflector and a time-of-flight mass spectrometer (TOFMS); the molecular beam is produced by a laser vaporization source. *p*-Aminobenzonitrile (PABN), *m*-aminobenzonitrile (MABN), *p*-(dimethylamino)benzonitrile (PDMABN), and *m*-(dimethylamino)benzonitrile (MDMABN) were purchased from SIGMA (purity ≥ 98%). PABN and MABN were mixed with cellulose in a 1:3 ratio. For PDMABN, a natural desorption was observed using this ratio, without laser of vaporization. To avoid this phenomenon, we diluted the mixture and used a 1:500 ratio. The mixing was pressed under 10^4 bars in a cylindrical mold to form a solid rod. For MDMABN, the sample was liquid, and we mixed ∼30 μL of this sample with 600 mg of cellulose in an excess of acetone to obtain a good homogeneity of the mixture. After evaporation of acetone, we obtained a mixture containing MDMABN that was pressed to form the rod. The third harmonic of a Nd^{3+}:YAG laser was used for the ablation of the rod that was rotated and translated in a screw motion. A short pulse of helium gas, synchronized with the ablation laser, was supplied by a piezoelectric valve. At the exit of the source, the molecules were thermalized in a 5-cm-long and 3-mm-diameter chamber maintained at room temperature. A thermal molecular beam was produced without supersonic expansion. After collimation, the beam traveled through a 15-cm-long electric deflector. In the deflector, a molecule with an electric dipole moment $\vec{\mu}$ is submitted to an instantaneous force along the *Z* axis (*Z* is the direction of the electric field and of its gradient):

$$f = \vec{\mu}\frac{\partial \vec{F}}{\partial Z} \tag{1}$$

A deflection is produced which is proportional to the time-averaged value ($\langle \mu_Z \rangle$) in the deflector of the projection on the *Z* axis of the dipole. Beam profiles are analyzed 1.025 m after the deflector, with a time-of-flight mass spectrometer coupled to a position sensitive detector.[13]

* Author to whom correspondence should be addressed. E-mail: rantoine@lasim.univ-lyon1.fr.

10.1021/jp0614345 CCC: $33.50
Published on Web 07/29/2006

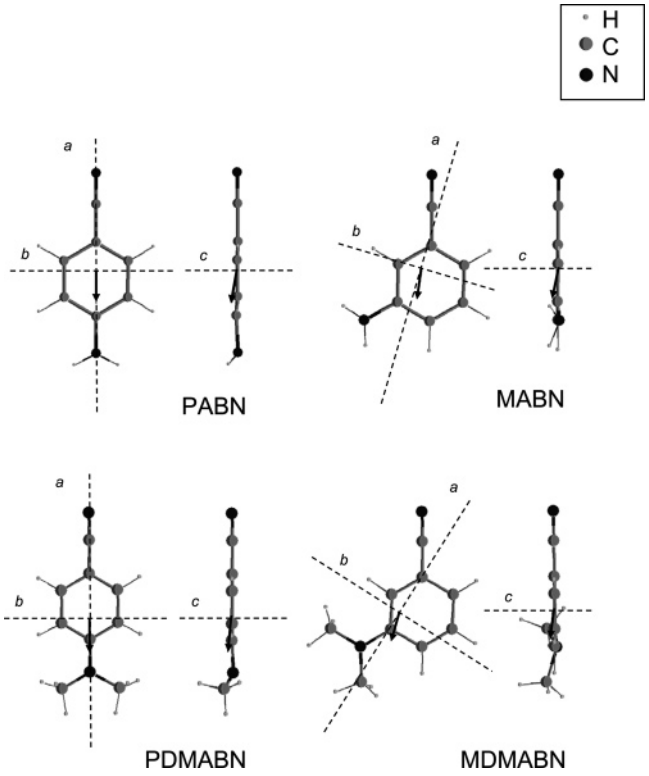

Figure 1. Geometry of the lowest energy conformation found at the MP2 6-311++G** level of theory for PABN and MABN molecules (chemical formula $H_2N-C_6H_4-CN$) and for PDMABN and MDMABN molecules (chemical formula $(CH_3)_2N-C_6H_4-CN$). The arrows show the direction and the relative magnitude of the electric dipole moment. The dashed lines display the direction of the principal axes of inertia in the plane of the benzene ring.

3. Structures, Electric Dipoles, and Internal Torsions. 3.1. Equilibrium Structures and Dipole Components. The ground-state geometry optimization was performed at the HF/MP2 level of theory. All the calculations were performed with Gaussian 98,[14] with the basis set 6-311++G**. The lowest energy structures for aminobenzonitrile molecules are displayed in Figure 1. For these molecules, the phenyl ring and the nitrile function are in the same plane, and the NH_2 group (for PABN and MABN) and the $N(CH_3)_2$ group (for PDMABN and MDMABN) are found out of plane. ABN molecules are polar molecules. The main component of the dipole lies along the principal *a*-axis. However, the nonplanar geometry gives rise to a non-null value of the dipole moment along the *c*-axis. For the *meta* isomers, in addition, there is a non-null value of the dipole moment along the *b*-axis. Rotational constants and dipole components are given in Table 1. These calculations can be compared to the values obtained for PABN and PDMABN by rotationally resolved spectroscopy.[15−17]An acceptable agreement between experiment and MP2 results is observed.

3.2. Internal Torsions. A strong vibration−rotation coupling can be induced by the activation of internal rotations at room temperature. Thus, a theoretical investigation has been undertaken to probe the energetics and the vibrational frequencies of the amine (NH_2) internal rotation for ABN molecules and of the methyl (Me) rotation and of the dimethyl amine ($N(Me)_2$) inversion and rotation for DMABN molecules. Labels for the internal rotations and for the corresponding angles are displayed in Figure 2. Energy barrier heights and harmonic frequencies of (NH_2), (Me), and ($N(Me)_2$) torsion modes were calculated for the equilibrium geometries, using Gaussian 98[14] and the graphical user interface Gabedit,[18] with the basis set 6-311++G** at the MP2 level of theory. Frequencies were computed numerically. The results of the calculations are given in Table 2 and in Figure 3.

3.2.1. Internal Inversion Mode. The barrier height for the inversion was estimated by performing single-point energy calculations at the structure of the lowest energy and at the structure where the amine or the dimethyl amine group is in the plane of the benzene ring. The presence of methyl groups slightly lowers the barrier height and decreases significantly the vibration frequency. Consequently, the population of vibrational states with $v \geq 1$, at $T = 300$ K, increases from 4% for ABN to ∼30% for DMABN molecules.

3.2.2. Internal Rotation Modes. For methyl and amine internal rotations, single-point calculations were performed as a function of the angle of rotation. Data were then fitted by a potential function of the form

$$V = \frac{V_0}{2}(1 - \cos n\alpha) \qquad (2)$$

where V_0 is the barrier height, α is the angle of rotation (ϕ for the amine torsion or φ for the methyl torsion), and n is the number of minima ($n = 3$ for the methyl rotation and $n = 2$ for the amine or dimethyl amine rotation). For ($N(Me)_2$) internal rotation calculations, both methyl groups were frozen.

(Me) Rotation Mode. Figure 3a displays the total energy versus the torsion φ angle for PDMABN molecule. The calculations predict a rotational barrier of 1574 cm^{-1} for the methyl group. The corresponding harmonic frequency is 157 cm^{-1}. A similar barrier height and harmonic frequency are obtained for the MDMABN molecule (see Table 2). The calculated energy barrier for methyl rotation is higher than the recent experimental estimation (∼500 cm^{-1}).[17] The difference might be partly because the calculations have been done assuming that the second methyl group was frozen. A concerted motion may lower the barrier. The population for this mode may be underestimated.

(NH_2) and ($N(Me)_2$) Rotation Modes. Figure 3b displays the total energies versus the torsion ϕ angle for the PDMABN molecule. The corresponding harmonic frequency is 110 cm^{-1}. A similar frequency is obtained for MDMABN (see Table 2). For PABN and MABN molecules, this mode has a much higher harmonic frequency (respectively, 296 and 283 cm^{-1}). The presence of methyl groups strongly affects the vibration frequencies, and the population of vibrational states with $v \geq 1$, at $T = 300$ K, increases from ∼25% for ABN to ∼62% for DMABN molecules.

For PDMABN, the calculated harmonic frequency for the ($N(Me)_2$) internal rotation is in agreement with the estimated frequency of ∼50 cm^{-1} of Gibson et al.[12] obtained by laser-induced fluorescence spectroscopy. From the barrier value and the moment of inertia of the $N(CH_3)_2$ group, one can estimate this frequency using[19]

$$\varphi = 2\sqrt{V_2 I_F} \qquad (3)$$

where V_2 is the barrier height and $I_F = \hbar^2 I_a / 2I_\alpha(I_a - I_\alpha)$ (I_a is the moment of inertia of the whole molecule about the axis *a*, and I_α is the moment of inertia of the rotating group about its symmetry axis). We found harmonic frequencies of 74 and 504 cm^{-1}, respectively, for PDMABN and PABN molecules, in agreement with the harmonic frequencies directly obtained from the MP2 calculations and experiments.[11,12]

TABLE 1: Relative Energies, Rotational Constants, Asymmetry Parameter $\kappa = (2B - A - C)/(A - C)$, and Calculated Electric Dipole of PABN, MABN, PDMABN, and MDMABN Obtained at the MP2 Level of Theory

			rotational constants (cm^{-1}) and asymmetry parameter				dipole components (debye)			
	basis set	energy (Hartree)	*A*	*B*	*C*	κ	μ_a	μ_b	μ_c	μ total
PABN										
MP2	6-311++G**	−378.856758	0.18549	0.03270	0.02782	−0.94	5.94	0.00	1.03	6.03
experiment[a]			0.18610(2)	0.033032(6)	0.028066(6)		6.41(3)			
PDMABN										
MP2	6-311++G**	−457.2276383	0.11554	0.01920	0.01663	−0.95	6.81	0.00	0.29	6.82
experiment[b]			0.11575	0.01930	0.01667					
MABN										
MP2	6-311++G**	−378.8561397	0.1116	0.0400	0.02947	−0.74	−5.17	0.51	1.08	5.29
MDMABN										
MP2	6-311++G**	−457.2272304	0.06934	0.02444	0.018266	−0.76	5.56	1.49	0.4	5.77

[a] References 15, 16. [b] Reference 17.

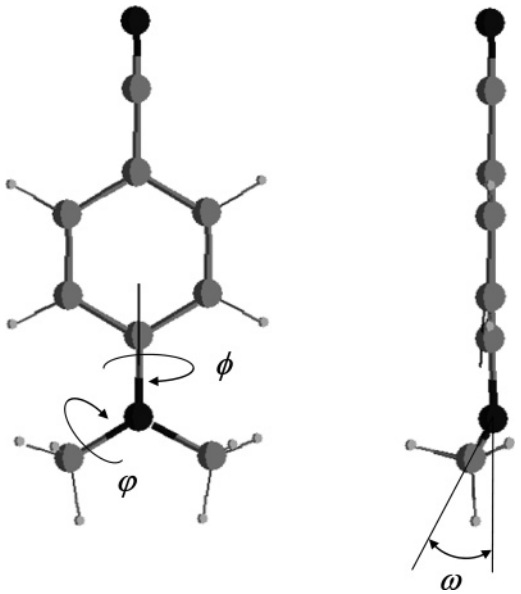

Figure 2. Definition of torsion angles for PDMABN. An analogous definition is used for the other compounds.

4. Simulations of Deflection Profiles. As described in our previous works,[5,20] electric deflection profiles can be simulated in two limiting cases: (i) rigid rotor and (ii) linear response theory.

4.1. Rigid Rotors. The Hamiltonian for a rigid rotor in an electric field may be written (the effect of the electronic polarizability is small and for simplicity is not included in eq 4) as

$$H = H_{\text{rot}} + H_{\text{Stark}} = AJ_a^2 + BJ_b^2 + CJ_c^2 - F_Z \sum_{g=a,b,c} \mu_g \phi_{Zg} \tag{4}$$

where *a*, *b*, and *c* are the principal axes of inertia of the rotor; J_a, J_b, and J_c are the corresponding components of the angular momentum; and *A*, *B*, and *C* are the rotational constants. *Z* has been chosen as the field direction in a laboratory fixed coordinate frame, μ_g is the components of the dipole moment along the principal inertial axes, and ϕ_{Zg} is the direction cosine or projection of the various molecular axes onto the field direction *Z*.

For an asymmetric rigid rotor, the eigenvalues of the Hamiltonian *H* are obtained by numerical diagonalization of the corresponding matrix on the basis of the eigenvectors of the prolate symmetric rotor. Profiles of deflection are calculated numerically from the derivatives of the energy eigenvalues as a function of the electric field, assuming that the molecules adiabatically enter the electric field. The result is a broadening of the molecular beam. This quantum mechanical approach is described in detail in paper I.[9] Simulations are done using rotational constants and dipole moment components given by MP2 calculations.

4.2. Linear Response. When couplings to rotation cannot be neglected, the motion of the molecule is no longer described by eq 4. In general, the calculation of the average value of the projection of the dipole on the axis of the electric field is not possible. However, when the correlation of the dipole on the axis of the electric field tends toward zero as the molecules travel through the deflector, $\langle \mu_Z(t=0)\mu_Z(t)\rangle \xrightarrow{t\to\infty} 0$ (i.e., a loss of memory of the orientation of the rotational motion), and assuming a canonical distribution before the molecules enter the deflector, the average value of the dipole on the axis of the electric field $\langle \mu_Z \rangle$ is the same for all the molecules and is given by the linear response theory:[21,22]

$$\langle \mu_Z \rangle = \left(\frac{\langle \mu^2 \rangle_{F=0}}{3kT} + \alpha \right) F \tag{5}$$

where $\langle \mu^2 \rangle_{F=0}$ is the average value of the square dipole of the molecule calculated at equilibrium without the electric field (at temperature $T = 300$ K) and α is the static electronic polarizability. In this case, beam profiles are globally deflected toward the high field region with a deflection *d* given by

$$d = \frac{K}{mv^2} \langle \mu_Z \rangle \frac{\partial F}{\partial Z} \tag{6}$$

where *K* is a geometrical constant, and *m* and *v* are the mass and the velocity of the molecule.

5. Results and Discussion. Figure 4 displays the experimental beam profiles recorded for PABN, MABN, PDMABN, and MDMABN molecules at $F = 0$ V/m and at $F = 0.61 \times 10^7$ V/m in the electric deflector. Beam profiles of PABN, MABN, and PDMABN in the presence of the electric field are different from the one of MDMABN. While an almost symmetric broadening is observed for PABN, MABN, and PDMABN, a global deflection with almost no broadening is observed for MDMABN. Profiles were systematically recorded as a function of the electric field inside the deflector from $F = 0$ V/m to $F = 1.21 \times 10^7$ V/m. In Figure 5, we have plotted the variation in the intensity of the signal at the maximum of the peak (I/I_0) as a function of the electric field *F* for PABN, MABN, PDMABN, and MDMABN molecules. This relative intensity is a measure of the broadening of the beam.

TABLE 2: Results of Calculations for the Barrier Heights and for the Harmonic Vibrational Frequencies for the Amine (NH_2) Rotation and Inversion for the Ground State of PABN and MABN Molecules, Dimethyl Amine ($N(Me)_2$) Rotation and Inversion and Me Rotation for the Ground State of PDMABN and MDMABN Molecules[a]

	NH_2 or $N(Me)_2$ inversion			NH_2 or $N(Me)_2$ rotation			Me rotation		
molecule	barrier height (cm^{-1})	harmonic vibration (cm^{-1})	vibration pop. $v \geq 1$ (%)	barrier height (cm^{-1})	harmonic vibration (cm^{-1})	vibration pop. $v \geq 1$ (%)	barrier height (cm^{-1})	harmonic vibration (cm^{-1})	vibration pop. $v \geq 1$ (%)
PABN	3857	666	4.1	2165	296	24.2			
MABN	3881	674	2.1	2302	283	25.7			
PDMABN	3600	299	23.8	2750	110	59.0	1574	157	47.1
MDMABN	3711	246	30.7	2631	90	64.9	1459	166	45.1

[a] The population of vibrational states with $v \geq 1$, at $T = 300$ K, is also given for each mode.

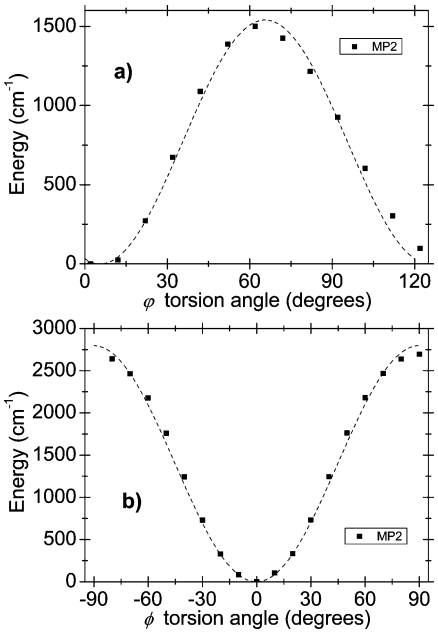

Figure 3. (a) MP2 relative energy of ground-state PDMADN versus φ torsion angle. (b) MP2 relative energy of ground-state PDMADN versus ϕ torsion angle. Simulations using a potential given by eq 2 are displayed in dashed lines.

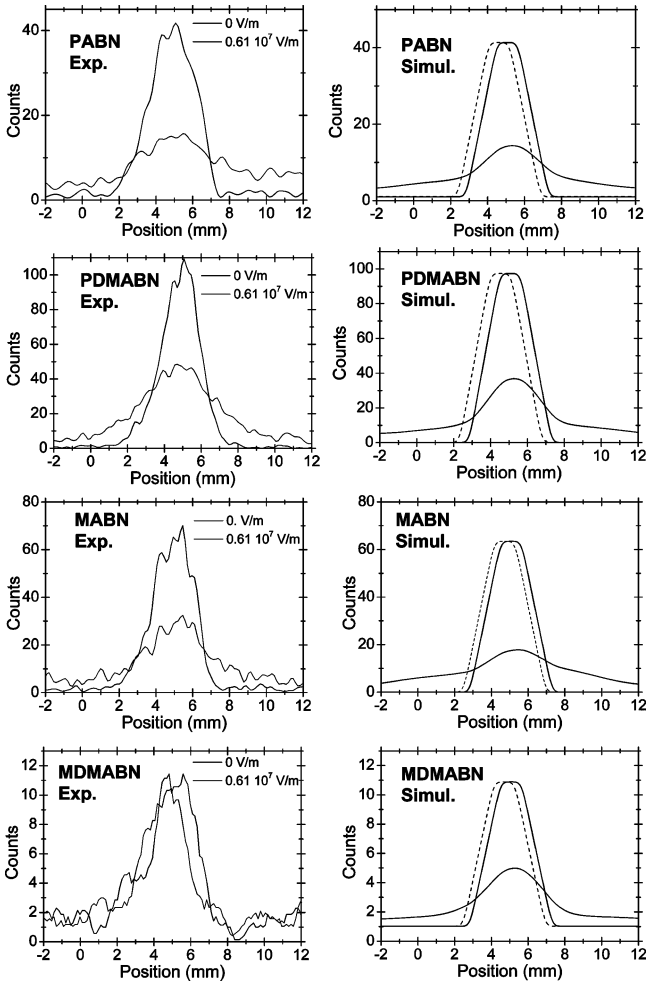

Figure 4. (left) Experimental beam profiles of ABN and DMABN molecules obtained at $F = 0$ V/m and at $F = 0.61 \times 10^7$ V/m in the deflector. (right) Simulated beam profiles of ABN and DMABN molecules obtained at $F = 0$ V/m and at $F = 0.61 \times 10^7$ V/m using the rigid rotor (solid line) and the linear response (dashed line) approaches. Molecular constants given in Table 1 were used for the simulations.

Experimental results are compared to simulations for rigid rotors (section 4.1) and to simulations using the linear response (section 4.2). For PABN, a good agreement between experiment and rigid rotor simulations is observed. For MABN and PDMABN, slight deviations between simulations and experiments are observed, especially at electric fields higher than 0.6×10^7 V/m (see Figure 5). The differences between the rigid rotor simulations and experiments are dramatic for MDMABN. The deflection observed for MDMABN is not reproduced by the Stark effect calculated for the rigid rotor. We interpret this as the signature of rotation−vibration couplings. The molecules are almost all deflected by the same amount, and deflection profiles can be simulated using the linear response (cf. Figure 4). Figure 6 displays for MDMABN molecules the evolution of the measured deflection (difference between the maximum of the peaks with and without F) as a function of the square of the electric field in the deflector. A linear behavior is observed. Results are in close agreement with the prediction of the linear response theory (eqs 5 and 6) using the MP2 calculated dipole value of 5.77 D (dashed line in Figure 6). A linear fit of the data leads to $\mu = 6.2 \pm 0.6$ D (straight line in Figure 6), taking $\alpha = 17.1$ Å^3 (value obtained at the HF/6-311++G** level of calculation).

To summarize, deflections of PABN molecules are described with rigid rotor simulations while the deflections of MDMABN molecules are described by the linear response theory. The differences between these molecules are the symmetry and the addition of methyl groups. In our previous paper, we have demonstrated that the rotation is chaotic for asymmetric molecules in external electric fields. The chaotic behavior can be quantified by a Brody statistical analysis.[9,23] The statistical parameter q of the Brody distribution is used as a measure of the intensity of the chaotic behavior of a quantum system ($q = 0$ for a nonchaotic Poisson distribution and $q = 1$ for a chaotic Wigner distribution). An analysis similar to the one performed on ABN molecules was performed on DMABN molecules (cf. Appendix I of ref 9 for the details of the analysis). Results of this analysis are displayed in Figure 7. They show that PABN

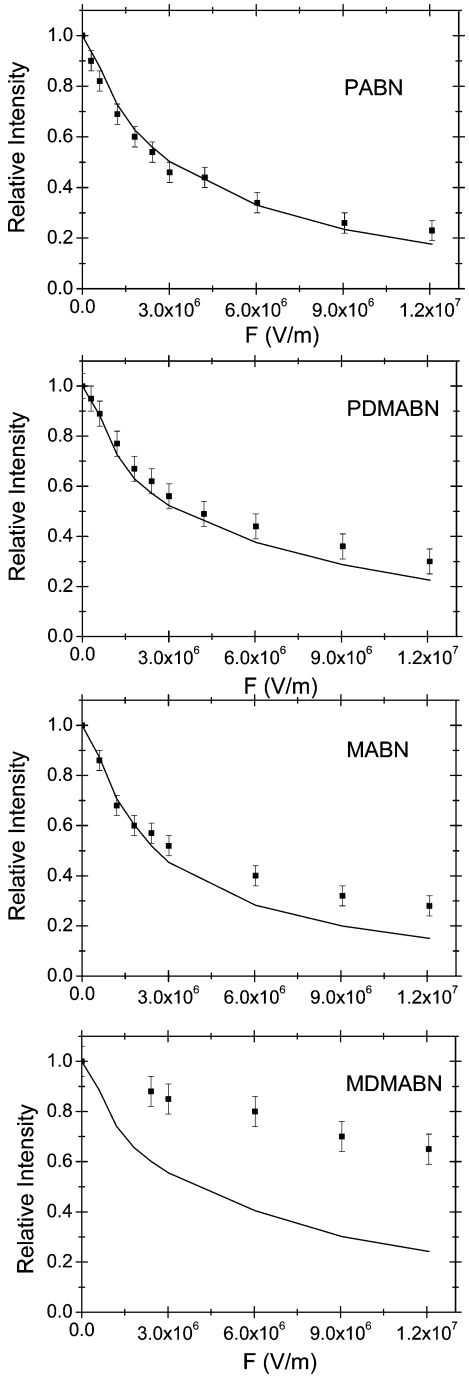

Figure 5. Relative intensity of the beam profile at its maximum intensity as a function of the electric field *F*. Squares correspond to experimental data and the lines correspond to the rigid rotor simulations. Molecular constants given in Table 1 were used for the simulations.

and PDMABN symmetric molecules have the same degree of chaotic behavior, while as expected, MABN and in particular MDMABN asymmetric molecules are much more chaotic.

A chaotic motion means that any perturbation can prompt a significant change in the rotational trajectories and can induce a modification in the average projection of the dipole moment. In paper I, this perturbation was induced by collisions with other particles (in particular, by addition of buffer gas in the deflector). In the present study, the collision effects were minimized, and they cannot explain the deviations observed between the rigid rotor simulations and the experiments. The introduction of methyl groups in ABN molecules induces some soft vibration modes which are populated at room temperature (cf. Table 2).

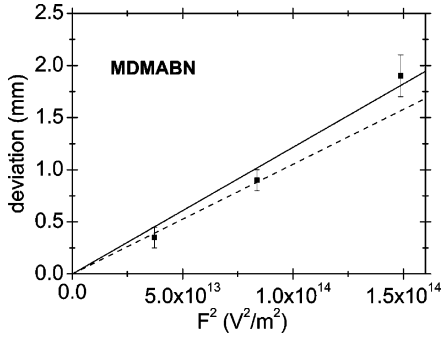

Figure 6. Deflection of the beam as a function of the square of the electric field for MDMABN. The dashed line is the prediction of the linear response theory (see eq 5) obtained using the calculated dipole value $\mu = 5.77$ D and taking $\alpha = 17.1$ Å^3. The solid line corresponds to a linear fit of the data leading to the experimental dipole value $\mu = 6.2 \pm 0.6$ D.

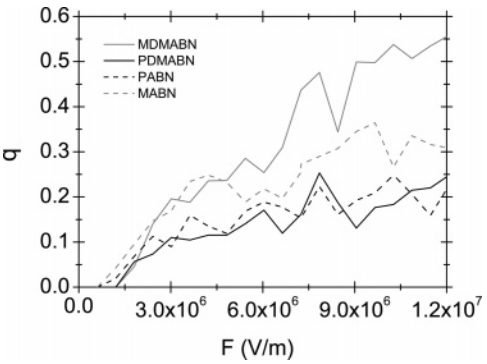

Figure 7. Evolution of the Brody parameter *q* as a function of *F* for ABN (dashed line) and DMABN (straight line) molecules for $M = 1$. The first 1500 levels were used to determine the Brody parameter.

Indeed, from our vibration analysis, we see that the $N(Me)_2$ torsion modes (both inversion and rotation) are populated for DMABN molecules. These modes could induce a strong coupling between the torsion of the $N(Me)_2$ group and the rotation of the whole molecule and therefore could affect deflection. Even if the number of populated vibrational states is low, this coupling may be particularly enhanced in the MDMABN molecules because of the repartition of rotation levels and the strong chaotic behavior of its rotational motion in electric fields. Influence of rotation−vibration couplings on electric deflections was previously described by Farley and coworkers[4,10] for hot benzene or toluene derivative molecules. In their work, with high-temperature heavy molecules ($T > 1000$ K), the density of vibrational states was about $>10^7$/cm^{-1}. In this high-state density regime, stationary states are irrelevant because they are mixed over the time scale of the experiment. In the present work, only ∼10 different vibrational states are populated for MDMABN. Because of the chaotic behavior of the rotation motion of the molecule, the coupling with a low number of vibrational states is, however, sufficient to induce a perturbation of this motion.

6. Conclusion. Our main point, in this article, is that the rotational motion of an asymmetric rotor in an external field is chaotic. Any perturbation, here vibration−rotation couplings, can lead to significant changes in the rotational motion. The changes explain the observation of the global shift of the beam in deflection experiments, while simulations for a rigid rotor predict a broadening of the beam.

References and Notes

(1) Friedrich, B.; Herschbach, D. R. *Comments At. Mol. Phys.* **1995**, *32*, 47.

(2) Loesch, H. J. *Annu. Rev. Phys. Chem.* **1995**, *46*, 555.
(3) Parker, D. H.; Bernstein, R. B. *Annu. Rev. Phys. Chem.* **1989**, *40*, 561.
(4) Farley, F. W.; McClelland, G. M. *Science* **1990**, *247*, 1572.
(5) Broyer, M.; Antoine, R.; Benichou, E.; Compagnon, I.; Dugourd, P.; Rayane, D. *C. R. Physique* **2002**, *3*, 301.
(6) Knickelbein, M. B. *J. Chem. Phys.* **2004**, *121*, 5281.
(7) Xu, X.; Yin, S.; Moro, R.; de Heer, W. A. *Phys. Rev. Lett.* **2005**, *95*, 237209/1.
(8) Amirav, A.; Navon, G. *Phys. Rev. Lett.* **1981**, *47*, 906.
(9) Abd El Rahim, M.; Antoine, R.; Broyer, M.; Rayane, D.; Dugourd, P. *J. Phys. Chem. A* **2005**, *109*, 8507.
(10) Farley, F. W.; Novakoski, L. V.; Dubey, M. K.; Nathanson, G. M. *J. Chem. Phys.* **1988**, *88*, 1460.
(11) Gibson, E. M.; Jones, A. C.; Phillips, D. *Chem. Phys. Lett.* **1988**, *146*, 270.
(12) Gibson, E. M.; Jones, A. C.; Bouwman, A. G. T. G.; Phillips, D.; Sandell, J. *J. Phys. Chem.* **1988**, *92*, 5449.
(13) Abd El Rahim, M.; Antoine, R.; Arnaud, L.; Barbaire, M.; Broyer, M.; Clavier, C.; Compagnon, I.; Dugourd, P.; Maurelli, J.; Rayane, D. *Rev. Sci. Instrum.* **2004**, *75*, 5221.
(14) Frisch, M. J.; Trucks, G. W.; Schlegel, H. B.; Scuseria, G. E.; Robb, M. A.; Cheeseman, J. R.; Zakrzewski, V. G.; Montgomery, J. A., Jr.; Stratmann, R. E.; Burant, J. C.; Dapprich, S.; Millam, J. M.; Daniels, A. D.; Kudin, K. N.; Strain, M. C.; Farkas, O.; Tomasi, J.; Barone, V.; Cossi, M.; Cammi, R.; Mennucci, B.; Pomelli, C.; Adamo, C.; Clifford, S.; Ochterski, J.; Petersson, G. A.; Ayala, P. Y.; Cui, Q.; Morokuma, K.; Malick, D. K.; Rabuck, A. D.; Raghavachari, K.; Foresman, J. B.; Cioslowski, J.; Ortiz, J. V.; Baboul, A. G.; Stefanov, B. B.; Liu, G.; Liashenko, A.; Piskorz, P.; Komaromi, I.; Gomperts, R.; Martin, R. L.; Fox, D. J.; Keith, T.; Al-Laham, M. A.; Peng, C. Y.; Nanayakkara, A.; Gonzalez, C.; Challacombe, M.; Gill, P. M. W.; Johnson, B.; Chen, W.; Wong, M. W.; Andres, J. L.; Gonzalez, C.; Head-Gordon, M.; Replogle, E. S.; Pople, J. A. *Gaussian 98*, revision A.7 ed.; Gaussian, Inc.: Pittsburgh, PA, 1998.
(15) Borst, D. R.; Korter, T. M.; Pratt, D. W. *Chem. Phys. Lett.* **2001**, *350*, 485.
(16) Berden, G.; van Rooy, J.; Meerts, W. L.; Zachariasse, K. A. *Chem. Phys. Lett.* **1997**, *278*, 373.
(17) Nikolaev, A. E.; Myszkiewicz, G.; Berden, G.; Meerts, W. L.; Pfanstiel, J. F.; Pratt, D. W. *J. Chem. Phys.* **2005**, *122*, 084309.
(18) Gabedit is a graphical user interface for Gaussian, Molpro, Molcas, and MPQC ab initio programs available from http://lasim.univ-lyon1.fr/allouche/gabedit.
(19) Lin, C. C.; Swallen, J. D. *Rev. Mod. Phys.* **1959**, *31*, 841.
(20) Antoine, R.; Compagnon, I.; Rayane, D.; Broyer, M.; Dugourd, P.; Breaux, G.; Hagemeister, F. C.; Pippen, D.; Hudgins, R. R.; Jarrold, M. F. *Eur. Phys. J. D* **2002**, *20*, 583.
(21) Van Vleck, J. H. *Phys. Rev.* **1927**, *30*, 31.
(22) Debye, P. *Polar Molecules*; Dover: New York, 1929.
(23) Brody, T. A.; Flores, J.; French, J. B.; Mello, P. A.; Pandey, A.; Wong, S. S. M. *Rev. Mod. Phys.* **1981**, *53*, 385.